Degradation Mechanism and Kinetics of Thermosensitive Polyacrylamides Containing Lactic Acid Side Chains

D. Neradovic, M. J. van Steenbergen, L. Vansteelant, Y. J. Meijer, C. F. van Nostrum, and W. E. Hennink*

Department of Pharmaceutics, Utrecht Institute for Pharmaceutical Sciences (UIPS), Faculty of Pharmaceutical Sciences, Utrecht University, P.O. Box 80082, 3508 TB Utrecht, The Netherlands

Received March 26, 2003; Revised Manuscript Received July 10, 2003

ABSTRACT: Diblock copolymers of poly(*N*-isopropylacrylamide-*co*-*N*-(2-hydroxypropyl)methacrylamide lactate) (poly(NIPAAm-*co*-HPMAm-lactate)) as a thermosensitive block and poly(ethylene glycol) (PEG) as a hydrophilic block form polymeric micelles above the cloud point (CP) of the temperature-sensitive block. Destabilization of these micelles occurs upon hydrolysis of the lactate side chains. Here we report on the degradation kinetics of the HPMAm-mono(di)lactate monomers and their copolymers with NIPAAm. The degradation of the monomers and polymers in their soluble state (thus below their CP) followed normal ester hydrolysis behavior: the degradation rate increased with temperature, pH (from pH 7.5 to 11), and dielectric constant of the medium. Above the CP, where the polymers are in a precipitated state, a significant retardation of the polymer degradation occurred due to a decrease of dielectric constant of the local environment of the precipitated polymer. This study shows that it is possible to predict the rate of formation of HPMAm in NIPAAm-*co*-HPMAm-lactate copolymers which results in an increase of the overall hydrophilicity of the polymers and destabilization of polymeric micelles based on poly(NIPAAm-*co*-HPMAm-lactate).

Introduction

During the past two decades, thermosensitive polymers have been intensively investigated as candidate biomaterials and drug delivery systems.[1−6] Among them, poly(*N*-isopropylacrylamide) (PNIPAAm) and its (block) copolymers have been the most extensively studied materials.[7−13] PNIPAAm is known for its unique thermally reversible solubility in aqueous solutions. It exhibits a lower critical solution temperature (LCST) behavior in water; i.e., it is soluble in water at temperatures lower than its cloud point (CP), but this polymer precipitates above this temperature.[14−17] This reversible hydration−dehydration behavior occurs in a narrow temperature range (30−33 °C in water).[18]

In a previous paper,[19] we reported the synthesis of copolymers containing NIPAAm and the lactic esters of (2-hydroxyethyl)methacrylic acid (HEMA-lactate), a new type of thermosensitive polymer with hydrolyzable lactate ester side groups. These random copolymers have a CP below that of PNIPAAm, which increases due to the hydrolysis of the hydrophobic lactate ester side groups. The resulting polymers poly(NIPAAm-*co*-HEMA) have a final CP independent of their composition of approximately 31 °C. Polymers whose CP would pass 37 °C (body temperature) during hydrolysis of the side groups would be much more attractive for the development of for example new drug delivery systems. We therefore synthesized a thermosensitive copolymer of NIPAAm and *N*-(2-hydroxypropyl)methacrylamide lactate (HPMAm-lactate). Poly(NIPAAm-*co*-HPMAm-lactate) with ≥35 mol % HPMAm-lactate has a CP well below body temperature and converts into poly(NIPAAm-*co*-HPMAm) with a CP above 37 °C upon hydrolysis.[20] Amphiphilic block copolymers form polymeric micelles in aqueous solution.[21−25] It has been shown that block and graft copolymers composed of a hydrophilic chain (e.g., poly(ethylene glycol) (PEG) or dextran) and a thermosensitive PNIPAAm chain form temperature-sensitive polymeric micelles, meaning that below the CP of PNIPAAm these polymers are soluble in water whereas they organize themselves in self-assembled structures (micelles) due to collapse of the PNIPAAm block above this temperature.[26−30] These colloidal particles, however, do not destabilize at physiological temperature. Therefore, we recently described a novel system based on diblock copolymers of poly(NIPAAm-*co*-HPMAm-lactate) and PEG.[20] These polymers self-assemble into nanosized particles at physiological temperature. During hydrolysis of the lactate acid side groups the cloud point increases, resulting in destabilization of the particles once the cloud point of the thermosensitive block passes 37 °C. It is expected when the particles are loaded with a drug, this destabilization process will be associated with release of the drug. Therefore, it is very important to have insight into the degradation kinetics of the polymers.

In this paper we report on a detailed study of the degradation kinetics of HPMAm-di/monolactate monomers and their copolymers with NIPAAm.

Experimental Section

1. Materials. 1,4-Dioxane (99+%, Fluka Chemie AG) was purified by distillation. The other chemicals were used as received. L-Lactide ((3*S*-*cis*)-3,6-dimethyl-1,4-dioxane-2,5-dione, >99.5%) was obtained from Purac Biochem BV (Gorinchem, The Netherlands). α,α′-Azoisobutyronitrile (AIBN), poly(ethylene glycol) 5000 monomethyl ether (PEG 5000), and dimethyl sulfoxide (DMSO) (puriss) were from Fluka Chemie AG (Buchs, Switzerland), and *N*-(2-hydroxypropyl)methacrylamide (HPMAm) was from Polysciences, Inc. (Brunschwig chemie, Warrington, PA). Stannous 2-ethylhexanoate (approximately 95%, $SnOct_2$) was from Sigma Chemical Co. (St. Louis, MO), and 4-methoxyphenol (99%) was from Janssen Chimica (Geel, Belgium). *N*-Isopropylacrylamide (NIPAAm,

* To whom correspondence should be addressed: tel +31-30 2536964, fax +31-302517839; e-mail W.E.Hennink@pharm.uu.nl.

10.1021/ma034381n CCC: $25.00
Published on Web 09/06/2003

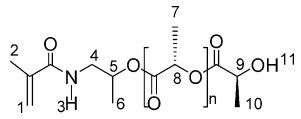

Figure 1. Structure of *N*-(2-hydroxypropyl)methacrylamide lactate (HPMAm-lactate).

97%) was obtained from Aldrich-Chemie (Steinheim, Germany).

Lactoyl lactate was synthesized, as will be reported in detail elsewhere.[31] In short, lactide was reacted with *sec*-phenethyl alcohol to yield *sec*-phenethyl lactoyl lactate. Next, this compound was converted quantitatively into the linear dimer of lactic acid, lactoyl lactate.

2. Methods. 2.1. ^{1}H NMR Spectroscopy. ^{1}H NMR spectra were recorded with a Gemini 300 MHz spectrometer (Varian Associates Inc. NMR Instruments, Palo Alto, CA). Spectra were obtained with or without TFAA (trifluoroacetic anhydride, 99+%) as a shifting reagent. With DMSO-d_6 as the solvent the central line of DMSO at 2.50 ppm was used as the reference line. With $CDCl_3$ as the solvent the $CHCl_3$ signal at 7.26 ppm was used as the reference line.

2.2. Synthesis of *N*-(2-Hydroxypropyl)methacrylamide Lactate (HPMAm-Lactate). HPMAm grafted with oligolactate (further abbreviated as HPMAm-lactate) was synthesized according to a slightly modified procedure previously reported.[32,33] In brief, a mixture of HPMAm (4.30 g, 30 mmol), L-lactide (2.16 g, 15 mmol), and 4-methoxyphenol (a polymerization inhibitor, 0.3 mmol) was heated to 130 °C until the lactide was molten. Subsequently, a catalytic amount of stannous octoate ($SnOct_2$, 0.3 mmol) was added. The resulting mixture was stirred for 5 h at 130 °C and thereafter allowed to cool to room temperature.

HPMAm-mono(di)lactate was isolated from the crude reaction mixture by preparative HPLC. Therefore, 1 g of the polydisperse product was dissolved in 200 μL of acetonitrile and then diluted with 800 μL of water. The resulting solution was centrifuged at 13 000 rpm for 5 min. After filtration through 0.45 μm polypropylene filters (Poly Pure filters 4 mm, Alltech), the solution was applied onto a preparative HPLC column.[34] A gradient was run from 80% A (water/acetonitrile = 5/95 (w/w)) to 100% B (water/acetonitrile = 95/5 (w/w)) in 40 min. The flow rate was 10 mL/min. UV detection at a wavelength of 250 nm was applied, and the individual peaks were collected. The collected products were freeze-dried and analyzed by ^{1}H NMR and by RP-HPLC (purity > 98%).

^{1}H NMR ($CDCl_3$) (see Figure 1): HPMAm-monolactate: δ 6.30 (b, 1H, H_3), 5.63 (s, 1H, H_1), 5.30 (s, 1H, $H_{1'}$), 5.09 (q, 1H, H_8), 4.24 (q, 1H, H_5), 3.55−3.35 (m, 2H, H_4), 1.92 (s, 3H, H_2), 1.35 (d, 3H, H_7) and 1.28 (d, 3H, H_6). HPMAm-dilactate: δ 6.25 (b, 1H, H_3), 5.70 (s, 1H, H_1), 5.35 (s, 1H, $H_{1'}$), 5.2−5.0 (m, 2H, H_8, H_9), 4.35 (q, 1H, H_5), 3.8−3.3 (m, 2H, H_4), 1.92 (s, 3H, H_2), 1.50 (d, 6H, H_7, H_{10}) and 1.27 (d, 3H, H_6).

3. Synthesis of Poly(NIPAAm-*co*-HPMAm-lactate). NIPAAm and HPMAm-mono(di)lactate were dissolved at a total monomer concentration of 0.1 g/mL in 1,4-dioxane. The monomer feed ratio was NIPAAm/HPMAm-mono(di)lactate = 65/35 (mol/mol). AIBN dissolved in 1,4-dioxane was added (total amount of monomers/initiator = 250/1 mol/mol), and the copolymerization was conducted at 60 °C for 20 h in a nitrogen atmosphere. Next, the solvent was removed under reduced pressure, and the copolymers were dissolved in acetone (around 20% (w/v)) and precipitated in an excess of diethyl ether. The precipitated polymers were isolated by filtration and dried in a vacuum oven at 40 °C.

^{1}H NMR for the dilactate containing polymer ($CDCl_3$; Figure 2): δ 6.55 (b, H_3, H_9), 5.35−4.8 (H_{13}, H_{15}), 4.41 (b, H_{12}), 3.95 (b, H_4), 3.42−3.75 (b, H_{10}), 2.62−0.6 (other protons). The comonomer ratio (mol/mol) in the copolymer was determined from the ratio of the integral of the methine proton (H_4) of NIPAAm to the integral of the methine (H_{12}) proton of HPMAm (see Figure 2).

2.4. Synthesis of Poly(NIPAAm-*co*-HPMAm-mono(di)-lactate)-*b*-PEG 5000. Block copolymers with NIPAAm/HPMAm-mono(di)lactate (molar ratio 65/35) as thermosensitive block and PEG as hydrophilic block were prepared by radical copolymerization via a macroinitiator route.[20]

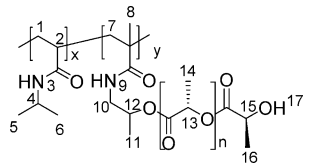

Figure 2. Structure of NIPAAm-*co*-HPMAm-lactate copolymers.

^{1}H NMR for the dilactate containing polymer ($CDCl_3$): δ 6.62 (b, H_3, H_9), 5.35−4.8 (b, H_{13}, H_{15}), 4.38 (b, H_{12}), 3.96 (b, H_4), 3.76−3.39 (b, PEG methylene protons CH_2−CH_2), 3.7−2.75 (b, H_{10}), 2.39−0.45 (the rest of the protons). The NIPAAm/HPMAm-lactate comonomer ratio (mol/mol) in the copolymer was determined as described above. The number-average molecular weight (M_n) of the thermosensitive block was determined by ^{1}H NMR as follows: (a) the value of the integral of the PEG protons divided by 454 (average number of protons per one PEG 5000 chain) gave the integral value for one PEG proton, and (b) the number of NIPAAm units in the polymers was determined from the ratio of the integral of the methine proton (H_4) of NIPAAm to the integral of one PEG proton. The ratio of the integral of the methine (H_{12}) proton of HPMAm to the integral value per one PEG proton gave the number of HPMAm-lactate units in the polymer. The number-average molecular weight of the NIPAAm-blocks was calculated from the resulting number of units.

2.5. Static Light Scattering (SLS). Static light scattering was measured as described previously.[19] In short, the copolymers were dissolved in 0.1 M PBS (pH = 7.2) at a concentration of 1 mg/mL. Onsets on the *x*-axis, obtained by extrapolation of the intensity−temperature curves to intensity zero, were considered as the cloud points (CP). The reported values are the averages of at least four measurements.

2.6. Degradation of the Monomers. Degradation of the monomers was investigated in 100 mM phosphate buffered saline (PBS), pH 7.5; the ionic strength (μ) was adjusted to 0.3 with NaCl. For other pH values, bicarbonate buffer (pH 8−9.2) and carbonate buffer (pH 10−11) were used (100 mM). For each study the pH of the buffer was adjusted at the temperature at which the study was conducted; the change in pH was less than 0.1 during the degradation studies. A 0.5 mL stock solution of HPMAm-mono(di)lactate in DMSO (2 mM) was diluted with 4.5 mL of buffer. Degradation reactions were carried out in glass bottles at various temperatures ranging from 15 to 60 °C. Samples (300 μL) were periodically drawn from the reaction mixtures and diluted with 700 μL of 1 M acetate buffer (pH 3.4) in order to stop further degradation. The samples were stored at 4 °C prior to HPLC analysis (see below). For each degradation curve at least six samples were drawn in a time frame corresponding with 1−3 half-lives. The interday variation in k_{obs} for HPMAm-dilactate was around 6% (k_{obs} at 60 °C and pH 7.5 was $(1.53 \pm 0.10) \times 10^{-4}$ s^{-1} ($n = 5$)).

2.7. Degradation of the Polymers. Degradation of poly(NIPAAm-*co*-HPMAm-monolactate) and poly(NIPAAm-*co*-HPMAm-dilactate) was investigated between 4 and 60 °C. Samples of 100 μL of the polymer solutions in water (10 mg/mL) were diluted with 100 μL of 300 mM sodium bicarbonate buffer of varying pH's (8, 9, and 10). The pH of the buffer was adjusted at the temperature of the study. At different time points, samples were taken, and 10 μL of 4 M HCl was added to adjust the pH to ~4 to stop further degradation. The samples were stored at −20 °C prior to the HPLC analysis (see below).

To determine the maximum amount of lactic acid which can be formed, hydrolysis was forced to completion by adding an equal volume of 0.1 M NaOH to a polymer solution followed by incubation at 60 °C for 17 h. The resulting reaction mixture was neutralized by adding 12.5 μL of 4 M HCl and stored at −20 °C prior to the HPLC analysis (see below).

Degradation of lactoyl lactate (concentration 1 mg/mL) was carried out at different temperatures (8−60 °C) and at pH 10. Analysis of the resulting degradation products was carried out under the same conditions as described for the polymers. Degradation of poly(NIPAAm-*co*-HPMAm-mono(di)lactate)-*b*-PEG 5000 was investigated at pH 10 and at 60 °C the same way as described above.

2.8. Degradation in Media with Different Dielectric Constants. Samples (60 μL) of stock solution of HPMAm-dilactate in DMSO (10 mM) were diluted to 3 mL with DMSO/sodium bicarbonate buffer mixtures. DMSO to buffer ratios of 10:90, 20:80, 30:70, 40:60, and 50:50 (v/v) were used (dielectric constant (ϵ) ranges from 76.8 to 63.4). Degradation was followed at 37 °C and at pH 9.2. The pH of every DMSO/buffer mixture was adjusted at the temperature of the study. Samples for the HPLC analysis were prepared the same way as described above.

2.9. Reversed-Phase High-Performance Liquid Chromatography (RP-HPLC). HPLC analysis of the samples was carried out on a Waters system (Waters Associates Inc., Milford, MA) consisting of a pump model 600, an autoinjector model 717, and a variable wavelength absorbance detector model 486. For the degradation studies of the monomers an analytical column LiChrosphere 100 RP-18 (5 μm, 125 × 4 mm i.d.) was used. For the degradation studies of the polymers an Alltech Prevail organic acid column (5 μm, 250 × 4.6 mm) was used. The flow rates were 1.0 mL/min, and the detection wavelength was 210 nm.

A gradient system was run for the analysis of HPMAm-mono(di)lactate, using methanol/water = 5/95 (w/w), pH 2 (eluent A) and methanol/water = 95/5 (w/w), pH 2 (eluent B). The pH of both eluents was adjusted by addition of perchloric acid. The gradient was run from 100% A to 100% B in 26 min. The injection volume was 100 μL. Calibration curves were generated for each monomer and its degradation products with freshly prepared standard solutions in 10 mM $HClO_4/H_2O$ (pH 2.4) in the appropriate concentration range. Peak areas were determined with Millennium 32 version 3.0 software (Waters Associates Inc.). The calibration curves for HPMAm-mono(di)-lactate and HPMAm were linear between 0.2 and 20 nmol.

For analysis of the amounts of lactic acid and lactoyl lactate, 25 mM KH_2PO_3 (pH 2.5) was used as eluent A and eluent B was acetonitrile/water = 95/5 (w/w). A gradient was run from 0% B to 60% B in 10 min, followed for 10 min by elution with 60% B. The injection volume was 50 μL. The calibration curves for lactic acid and lactoyl lactate were linear between 0.01 and 4 μmol.

2.10. Hydrolysis of the Ester Bond between the PEG and NIPAAm Blocks in the Block Copolymer. The block copolymer of NIPAAm and PEG 2000 (6800:2000 g/mol) was prepared by radical copolymerization using $(PEG\ 2000)_2$-ABCPA as initiator essentially as described previously.[20] The hydrolytic degradation of the ester bond between the blocks in the $PNIPAAm_{(M_n=6800)}$/PEG 2000 polymer was followed at 37 °C and at pH 8.5. For each study (n = 4), 100 μL polymer samples in water (concentration 40 mg/mL) were pipetted into the Eppendorf vials. Next, 900 μL of 0.1 M Tris buffer (pH 8.5) was added. The vials were placed in a water bath at 37 °C. At different time points vials were taken out of the water bath, and the pH was adjusted to ∼4 by addition of 18.5 μL of 4 M HCl. The samples were stored at 4 °C prior to analysis.

The formation of PEG 2000 in time was followed by gel permeation chromatography (GPC) using a model 600 HPLC pump, a model 410 differential refractometer (Waters Associates Inc., Milford, MA), and a PL-aquagel-OH mixed column (8 μm, Polymer Laboratories Inc., Amherst, MA). Filtered 0.1 M Tris buffer (pH 7.5) was used as the mobile phase. The analysis was conducted at 30 °C. The flow rate was 1 mL/min. For calibration of the column solutions of PEG 2000 monomethyl ether in eluent with known concentrations were used.

2.11. Predictive Value of the Kinetic Model. To demonstrate the predictive value of the kinetic model, the destabilization of nanoparticles based on poly(NIPAAm-*co*-HPMAm-dilactate (65/35 (mol/mol))-*b*-PEG 5000 at 37 °C and pH 5 and pH 10 was followed by dynamic and static light scattering measurements. In detail, the block copolymer was dissolved in water (2 mg/mL) at 4 °C (below the cloud point). The aqueous polymer solution was diluted with an equal volume of 0.3 M $NaHCO_3$ buffer pH 10 at 4 °C. Before the analysis the sample was filtrated through 0.4 mm nylon filters (Alltech Associates Inc., Deerfield, IL). A cuvette with the cold polymer solution was transferred to the heated cell holder of a spectrofluorometer at 37 °C. The light scattering by the polymer solution at 37 °C was measured in time at a wavelength of 650 ± 2.5 nm under a 90° angle. In a separate experiment, the particle size in time was monitored using DLS at 37 °C and at both pH 5 and pH 10. For the study at pH 5, 1 mg/mL of the polymer was dissolved in 0.15 M ammonium acetate buffer at 4 °C. The DLS cuvette with the copolymer solution was cooled to 4 °C and subsequently placed in the heated cell holder at 37 °C.

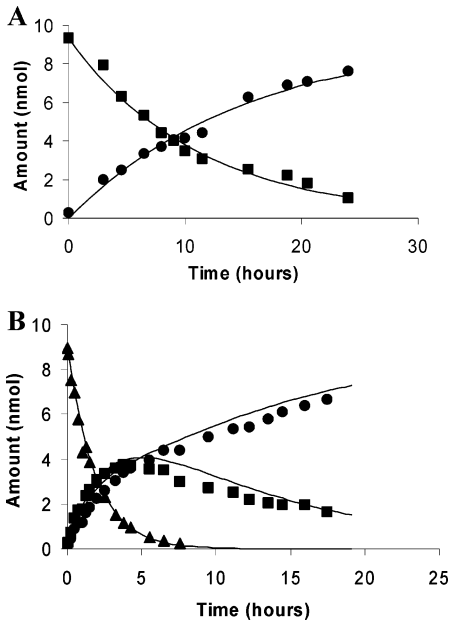

Figure 3. Degradation profiles of (A) HPMAm-monolactate and (B) HPMAm-dilactate at 60 °C at pH 7.5 (symbols represent the experimental data; drawn lines are fitted according to eqs 3−5): (▲) HPMAm-dilactate; (■) HPMAm-monolactate; (●) HPMAm.

Results

Degradation of the Monomers. The hydrolysis of HPMAm-mono(di)lactate was determined in the range 15−60 °C and at pH 7.5. At all temperatures the concentration of both monomers decreased according to pseudo-first-order kinetics. Typical degradation profiles of HPMAm-monolactate and HPMAm-dilactate at 60 °C and pH 7.5 are shown in parts A and B of Figure 3, respectively. The detected hydrolysis product of HPMAm-monolactate was HPMAm, while degradation of HPMAm-dilactate resulted in the formation of HPMAm-monolactate and HPMAm. In both cases no MAA was detected as a degradation product, which can be attributed to the high stability of the amide bond.

The observed first-order reaction rate constants (k_{obs}) at 37 °C and pH 7.5 are for HPMAm-monolactate (2.20 ± 0.06) × 10^{-6} s^{-1} ($t_{1/2}$ = 87.5 h) and for HPMAm-dilactate (1.25 ± 0.07) × 10^{-5} s^{-1} ($t_{1/2}$ = 15.4 h).

The pH dependence of k_{obs} for both HPMAm-monolactate and HPMAm-dilactate was studied in the pH range 7.5−11. k_{obs} can be described by the general rate constant equation (eq 1):

$$k_{obs} = k_0 + k_H[H^+] + k_{OH}[OH^-] \qquad (1)$$

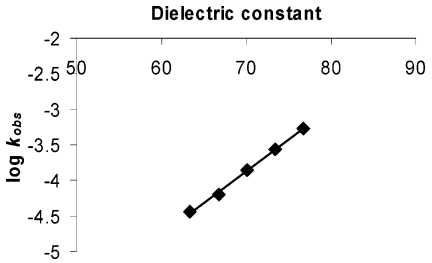

Figure 4. Influence of the dielectric constant (ϵ) on k_{obs} (pH 9.2, 37 °C).

Scheme 1. Possible Degradation Routes for the HPMAm-Mono(di)lactate Monomers (R Is HPMAm)

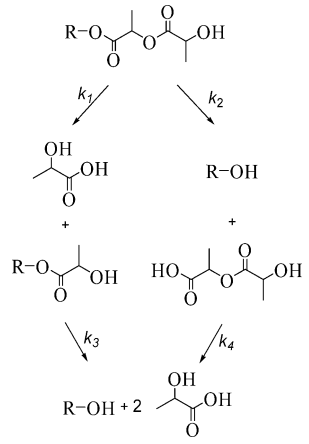

Table 1. Reaction Rate Constants for HPMAm-Dilactate at 37 °C (pH 7.5) in Water with 10% DMSO[a]

monomer	k_1 (h^{-1}) ± SD	k_2 (h^{-1}) ± SD	k_3 (h^{-1}) ± SD
HPMAm-dilactate	0.032 ± 0.002	0.014 ± 0.003	0.0079 ± 0.0002

[a] k_1, k_2, and k_3 refer to the reactions of Scheme 1.

In this equation k_0 is the first-order rate constant for the degradation in water only, while k_H and k_{OH} are second-order rate constants for degradation catalyzed by protons and hydroxyl ions, respectively. From the log k_{obs}–pH graphs for both HPMAm-monolactate and HPMAm-dilactate, it was concluded that in the pH range studied (pH 7.5–11) the slopes of the curves for both monomers approach +1 (results not shown), indicating that the hydrolysis of both monomers in the pH range investigated is specifically hydroxyl-catalyzed. This is in agreement with the results reported for other esters.[35–37]

The degradation rate of HPMAm-dilactate decreased with decreasing dielectric constant of the medium (Figure 4), as reported before for other esters.[36–38]

The two possible degradation routes of HPMAm-dilactate are shown in Scheme 1. The route shown on the left side of Scheme 1 is a consecutive first-order reaction of the formation and degradation of the monolactate. For this part of the reaction sequence the following rate equation is valid for the amount of monolactate present in the reaction mixture:[39]

$$[\mathrm{M-L}]_t = [\mathrm{M-LL}]_0 \frac{k_1}{k_3 - k_1}(e^{-k_1 t} - e^{-k_3 t}) \qquad (2)$$

where $[\mathrm{M-LL}]_0$ is the starting amount of HPMAm-dilactate and k_1 and k_3 are the rate constants as shown in Scheme 1. k_3 equals the before-mentioned k_{obs} of the degradation of HPMAm-monolactate. The fraction of molecules, which follows the route via the monolactate and not the one shown on the right side of Scheme 1, is equal to $k_1/(k_1 + k_2)$. Therefore, for the situation represented by Scheme 1, eq 2 becomes

$$[\mathrm{M-L}]_t = \frac{k_1}{k_1 + k_2}[\mathrm{M-LL}]_0 \frac{k_1}{k_3 - k_1}(e^{-k_1 t} - e^{-k_3 t}) \qquad (3)$$

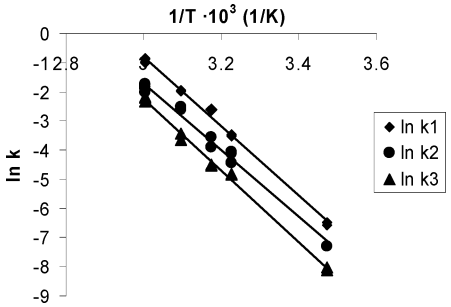

Figure 5. Arrhenius plots for degradation of HPMAm-mono-(di)lactate at pH 7.5.

From the decreasing amounts of HPMAm-dilactate in time an "overall rate constant" was determined (k_{obs}) that equals the sum of two reaction rate constants $k_1 + k_2$. The values of k_1 and k_2 were calculated by fitting the amount of monolactate (M–L) as a function of time using eq 3.

The measured amounts of HPMAm-dilactate $[\mathrm{M-LL}]_t$ and HPMAm ($[\mathrm{M}]_t$) were fitted to eqs 4 and 5:

$$[\mathrm{M-LL}]_t = [\mathrm{M-LL}]_0 e^{-(k_1+k_2)t} \qquad (4)$$

$$[\mathrm{M}]_t = [\mathrm{M-LL}]_0 - [\mathrm{M-LL}]_t - [\mathrm{M-L}]_t \qquad (5)$$

The calculated values for the reaction rate constants (Table 1) correspond well with the experimental data, as can be seen in Figure 3A,B.

By following the degradation of lactoyl lactate at different temperatures and at pH 10, the reaction rate constant k_4 as a function of temperature was determined.

The curve fittings were performed with the experimental data at every incubation temperature of HPMAm-mono(di)lactate (pH 7.5). Figure 5 shows the corresponding Arrhenius plot for the hydrolysis of HPMAm-mono(di)lactate. This figure shows that the activation energies for the three subreactions are equal (97 ± 5 kJ/mol).

Degradation of the Polymers. HPMA-monolactate and dilactate were used to prepare random copolymers with NIPAAm. NIPAAm/HPMAm-mono(di)lactate monomer feed ratios of 65/35 (mol/mol) were used. The copolymers were obtained in good yields (80–90%). As determined by ^{1}H NMR, the monomer ratio in poly(NIPAAm-*co*-HPMAm-monolactate) was 68/32 (mol/mol) and for poly(NIPAAm-*co*-HPMAm-dilactate) it was 69/31 (mol/mol). The cloud points were 31.5 and 18.7 °C, respectively; after hydrolysis the CP of the formed poly(NIPAAm-*co*-HPMAm) was 43.5 °C.

Two thermosensitive block copolymers, namely poly(NIPAAm-*co*-HPMAm-monolactate)-*b*-PEG 5000 and poly(NIPAAm-*co*-HPMAm-dilactate)-*b*-PEG 5000, were synthesized. The M_n of the thermosensitive block in the first polymer was 14 500, and the NIPAAm/HPMAm-monolactate ratio was 68/32 (mol/mol). Poly(NIPAAm-

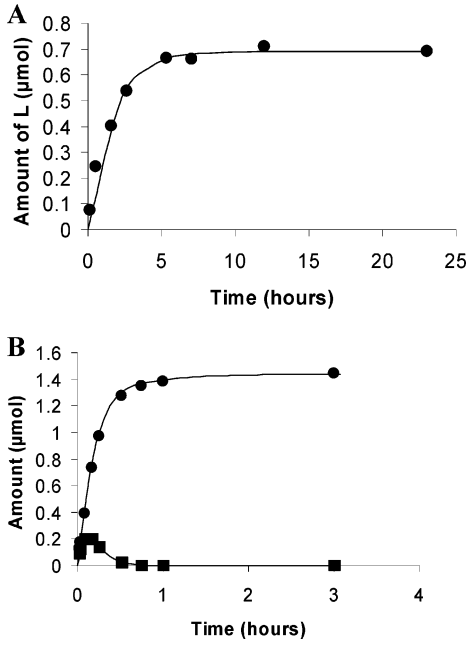

Figure 6. Degradation curves of (A) poly(NIPAAm-*co*-HPMAm-monolactate) at 25 °C and at pH 10 and (B) poly(NIPAAm-*co*-HPMAm-dilactate) at 60 °C and at pH 10 (symbols are experimental data; drawn lines are calculated by curve fitting according to the equation $[L]_t = [P-L]_0 e^{-k_3 t}$ for the polymer with HPMAm-monolactate[39] and eqs 6 and 8 for the polymer with HPMAm-dilactate): (■) lactoyl lactate; (●) lactic acid.

co-HPMAm-dilactate)-*b*-PEG 5000 had a $M_n = 10\,800$ for the thermosensitive block, and the NIPAAm/HPMAm-dilactate molar ratio was 73/27 (mol/mol). The CP of the block copolymers with the HPMAm-monolactate was 33.9 °C, while the CP of the block copolymers with the HPMAm-dilactate was 19.6 °C; after hydrolysis the CP was 44 °C.

Hydrolysis of the lactic acid side chains was followed by the formation of lactic acid and lactoyl lactate. Degradation of the polymers was done at temperatures between 4 and 60 °C (below and above the cloud point of the polymers) and at pH 10. Degradation of the poly(NIPAAm-*co*-HPMAm-monolactate) resulted in the formation of lactic acid (L) as degradation product, while during the degradation of poly(NIPAAm-*co*-HPMAm-dilactate) both L and LL (lactoyl lactate) were detected by HPLC. Typical degradation profiles for the polymers are shown in Figure 6.

The same degradation scheme, presented for the degradation of the monomers, can be applied for degradation of the polymers (Scheme 1, where R is the polymer backbone).

Knowing the values of the rate constants k_3 (0.052 min^{-1}, Figure 6A) and k_4 (see monomer degradation section), the measured amounts of L and LL formed during the degradation of poly(NIPAAm-*co*-HPMAm-dilactate) were fitted using the following equations (eq 6 and 7):

$$[LL]_t = \frac{k_2}{k_1 + k_2}[P-LL]_0 \frac{k_2}{k_4 - k_2}(e^{-k_2 t} - e^{-k_4 t}) \quad (6)$$

and

$$[L]_t = 2[P-LL]_0 - 2[P-LL]_t - [P-L]_t - 2[LL]_t \quad (7)$$

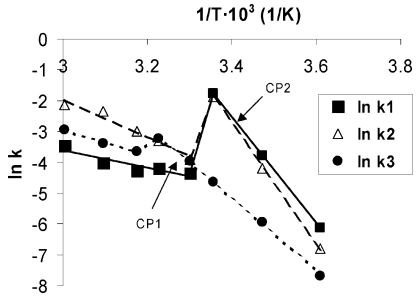

Figure 7. Arrhenius plot for poly(NIPAAm-*co*-HPMAm-mono-(di)lactate) at pH 10. CP1 and CP2 refer to the cloud points of the polymers with HPMAm-monolactate and HPMAm-dilactate before hydrolysis of the lactic acid side groups, respectively.

Equation 7 is derived knowing that the amount of free lactic acid ($[L]_t$) is equal to 2 times the amount of polymer-bound dilactate at $t = 0$ minus the amount of lactic acid still bound to the polymer or present as its dimer at time t. The total amount of lactic acid in the copolymer at $t = 0$ ($2[P-LL]_0$) is known from the composition of the polymer as determined by NMR (see above) and was checked by HPLC determination of the amounts of lactic acid produced after driving the hydrolysis to completion using 0.1 M NaOH at 60 °C. Combining eqs 3, 4 and 6 with eq 7 yield

$$[L]_t = [P-LL]_0\left\{2 - 2e^{-(k_1+k_2)t} - \left[\frac{k_1}{k_1 + k_2}\frac{k_1}{k_3 - k_1} \times (e^{-k_1 t} - e^{-k_3 t})\right] - 2\left[\frac{k_2}{k_1 + k_2}\frac{k_2}{k_4 - k_2}(e^{-k_2 t} - e^{-k_4 t})\right]\right\} \quad (8)$$

All variables in eqs 6 and 8 are known except for k_1 and k_2, which can be obtained by the curve fitting procedure as discussed earlier in this study. As can be seen in Figure 6, the fitted curves correspond very well to the experimental data. The Arrhenius plots for the polymers undergoing the reactions of Scheme 1 are shown in Figure 7. E_a for the polymer with HPMAm-monolactate below the cloud point (CP1 = 31.5 °C, Figure 7) is 95 ± 3 kJ/mol, and this value corresponds well with the activation energy of the hydrolysis of the monomer. No accurate values for the degradation reactions represented by k_1 and k_2 (Scheme 1) for the polymer with HPMAm-dilactate can be given because k values at only two temperatures below the CP (CP2, Figure 7) are available. Discontinuities in the Arrhenius plots (Figure 7) are clearly present around the cloud points of the polymers. Above the CP, E_a is 37 ± 13 kJ/mol for the three subreactions.

Table 2 shows the values of the reaction rate constants at pH 7.5 for poly(NIPAAm-*co*-HPMAm-dilactate) at 15 °C (below the CP) and 60 °C (above the CP). The reaction rate constants of the monomers under the same conditions are also given. The reaction rate constants for the polymer below its CP are of the same order of magnitude as those for the monomer, but above the CP the polymer degrades 1−2 orders of magnitude slower.

The influence of pH on the degradation of the poly(NIPAAm-*co*-HPMAm-mono(di)lactate) polymers was studied at 60 °C and at pH 8−10. The log k−pH profile shows that the degradation of poly(NIPAAm-*co*-HPMAm-mono(di)lactate) is OH^- catalyzed in this pH range, since the slope of the curve approaches +1 (results not shown).

Table 2. Reaction Rate Constants for the Hydrolysis of HPMAm-Dilactate and Poly(NIPAAm-*co*-HPMAm-dilactate) at pH 7.5

temp (°C)	reaction rate constant[a] (min^{-1})	HPMAm-dilactate[b]	poly(NIPAAm-*co*-HPMAm-dilactate)
15	k_1	4.8×10^{-5}	7.3×10^{-5}
	k_2	2.4×10^{-5}	4.7×10^{-5}
	k_3	1.0×10^{-5}	8.4×10^{-6}
	k_4	1.9×10^{-6}	1.9×10^{-6}
60	k_1	1.3×10^{-2}	9.9×10^{-5}
	k_2	5.3×10^{-3}	3.8×10^{-4}
	k_3	3.7×10^{-3}	1.6×10^{-4}
	k_4	4.7×10^{-4}	4.7×10^{-4}

[a] k_1, k_2, k_3, and k_4 refer to the reactions of Scheme 1. [b] Calculated reaction rate constants in water using the data of HPMAm-dilactate degradation in water/DMSO mixture (the presence of 10% DMSO in the degradation mixture decreased the degradation rate constants by a factor 2 (Figure 4)).

The degradation rate constants for the hydrolysis of HPMAm-lactate in the poly(NIPAAm-*co*-HPMAm-mono(di)lactate)-*b*-PEG 5000 diblock copolymers at 60 °C and pH 10 corresponded with those for random poly(NIPAAm-*co*-HPMAm-mono(di)lactate) copolymers: degradation rate constants were $k_1 = 0.032$ min^{-1}, $k_2 = 0.20$ min^{-1}, and $k_3 = 0.056$ min^{-1} (compare with $k_1 = 0.031$ min^{-1}, $k_2 = 0.12$ min^{-1}, and $k_3 = 0.052$ min^{-1} for the random polymers).

Since the blocks in the block copolymers are connected via a hydrolyzable ester bond, the hydrolysis rate of this bond was also determined. It was shown that, at pH 8.5 and at 37 °C, k_{obs} for the hydrolysis of this ester bond is $(3.4 \pm 0.3) \times 10^{-4}$ min^{-1} ($t_{1/2} = 34$ h). This means that the hydrolysis of the ester bond between the blocks proceeds almost 5 times slower as compared to the degradation rates of the lactic acid side groups.

Predictive Value of the Kinetic Model. To demonstrate the predictive value of the kinetic model, the destabilization of nanoparticles based on poly(NIPAAm-*co*-HPMAm-dilactate (65/35 (mol/mol)))-*b*-PEG 5000 at 37 °C and pH 5 and 10 was followed by dynamic and static light scattering measurements. The experimentally obtained destabilization time was compared with the calculated time as predicted by the kinetic model. Dynamic light scattering (DLS) at 37 °C and pH 5, i.e., under the conditions where hydrolysis of the polymer proceeds very slowly, showed that after 5 min incubation particles of 170 ± 5 nm and with a low polydispersity (PD $= 0.087 \pm 0.004$) were detected. During the next 60−70 min of incubation, the particles decreased in size to 152 ± 4 nm (PD $= 0.085 \pm 0.005$), which is likely due to a further dehydration of the hydrophobic core. After 24 h of incubation, nanoparticles with approximately the same particle size and polydispersity (159 ± 3 nm and PD $= 0.09 \pm 0.01$) were detected. This demonstrates that under conditions where degradation is minimized the particles are rather stable.

Destabilization of nanoparticles based on poly(NIPAAm-*co*-HPMAm-dilactate)-*b*-PEG 5000 was followed at 37 °C and pH 10 by DLS and SLS (Figure 8). Several stages in the destabilization process can be distinguished. After 5 min of incubation, particles of 190 ± 2 nm with a narrow size distribution (PD $= 0.083 \pm 0.003$) were observed in the opalescent polymer solution. During the next 10 min, both a slight decrease in the intensity of scattered light and a small but significant decrease in the particle size to 178 ± 3 nm were observed. Obviously, because of ongoing dehydration of the hydrophobic core of the nanoparticles, they become smaller, as observed for the nanoparticles incubated under conditions where degradation of the polymer is minimal (pH 5). During the next 15 min of incubation, both an increase of the intensity of the scattered light and the particle size (to 189 ± 3 nm, PD $= 0.08 \pm 0.02$) were observed. Likely, because of hydrolysis of the lactic acid side groups and the herewith associated increase in hydrophilicity of the polymer, the particles start to swell, resulting in an increasing particle size in time. The next phase (30−50 min) is characterized by a significant increase of the particle size and polydispersity as well as a gradual disappearance of the SLS signal. This substantial increase in particle size is due to the increasing hydrophilicity of the hydrophobic particle core caused by ongoing hydrolysis of the lactic acid ester groups. After 60 min, the polymer solution had a clear appearance. In agreement herewith, the SLS signal was low. These results indicate that between 50 and 60 min the destabilization of the polymeric nanoparticles was complete.

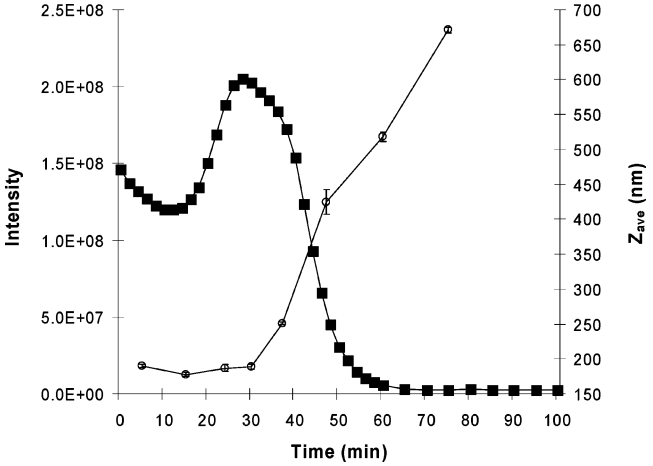

Figure 8. Incubation of poly(NIPAAm-*co*-HPMAm-dilactate)-*b*-PEG 5000 copolymer in 0.15 M $NaHCO_3$ buffer pH 10 and at 37 °C followed by SLS (■, intensity) and DLS (○, average particle size (Z_{ave})).

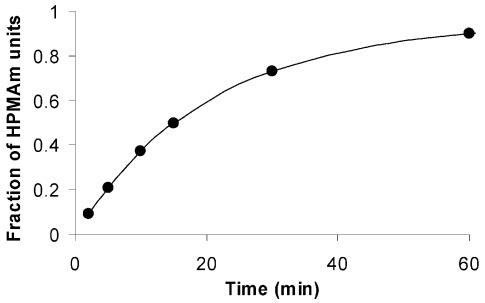

Figure 9. Formation of HPMAm units during degradation of poly(NIPAAm-*co*-HPMAm-dilactate)-*b*-PEG 5000 at 37 °C and pH 10, calculated according to eq 5.

The rate of formation of the HPMAm units during the polymer degradation can be calculated using eq 5 and the experimentally determined reaction rate constants for hydrolysis of the polymer containing di- and monolactic acid side groups. $[M]_t$ in eq 5 is equal to the amount of fully hydrolyzed HPMAm units, and $[M-LL]_0$ is the amount of the polymer bound dilactate at $t = 0$, while $[M-LL]_t$ and $[M-L]_t$ are the amounts of di- or monolactic acid still bound to the polymer at time t, calculated using eqs 4 and 3, respectively.

Figure 9 shows the calculated amount of HPMAm units during incubation at 37 °C and pH 10. It can be

seen that it takes about 1 h to hydrolyze about 90% of the side groups from the polymer. As demonstrated previously,[20] the block copolymer formed after hydrolysis (poly(NIPAAm-*co*-HPMAm 65/35) has a cloud point above 37 °C. This indicates that the kinetic model predicts that a soluble polymer is formed after 60 min. SLS and DLS measurements reveal that experimentally this conversion is found around 50−60 min, which is in excellent agreement with the calculated destabilization time.

Discussion

From the overall reaction rate constant (k_{obs}) values for HPMAm-mono(di)lactate, it is obvious that the monomer with two lactate groups hydrolyzes 6 times faster than the monomer with one lactate (compare k_1 plus k_2 with k_3; Table 1). We previously demonstrated that, during the degradation of a monodisperse lactic acid oligomer with a blocked carboxylic acid end group, preferentially lactoyl lactate was split off, which can be explained by intramolecular transesterification, also known as backbiting.[36] For HPMAm-dilactate the following order in the values of the constants was obtained: $k_1 > k_2 > k_3$ (Table 1). This indicates that in HPMAm-dilactate the different ester groups are not equally susceptible to hydrolysis. The ester group between the two lactate groups (k_1) is more sensitive for hydrolysis than the one between HPMAm and lactate (k_3). Nevertheless, the "backbiting" mechanism (k_2) still plays a role in the degradation of HPMAm-dilactate because the HPMAm-lactate ester bond in the dilactate (k_2) is hydrolyzed somewhat faster than the same ester bond in the monolactate (k_3).

The influence of the dielectric constant of the solvent on the monomer hydrolysis rates was determined for the following reason. The (NIPAAm-*co*-HPMAm-lactate) polymers are soluble in aqueous solutions below their cloud point, but above this temperature they become hydrophobic and precipitate. By this process the local environment of the precipitated polymers becomes hydrophobic and consequently has a lower dielectric constant. From Figure 4 it can be seen that, at a higher dielectric constant of the medium, the degradation proceeds faster. This is consistent with findings for the hydrolysis of (poly)esters[36−38] and can be explained by the fact that the organic solvent molecules stabilize the ground state more than the transition state, resulting in higher activation energy.

In contrast to the hydrolysis kinetics of the monomers, the Arrhenius plots for the hydrolysis of HPMAm-lactate based polymers (Figure 7) clearly show discontinuities around the CP of the polymer. Three separate regions can be distinguished, i.e., below the CP of the starting polymer, above the CP of the fully hydrolyzed polymer, and at intermediate temperatures. The degradation rate constants of the polymers below their CP's are almost equal to those for the monomers (Table 2). Below the cloud point, the polymer is completely dissolved and the polymer chains are fully hydrated. In this state the lactate ester groups are relatively easily accessible for hydrolysis. As for the monomers, the degradation of the ester bond between the two lactate groups (k_1) is the fastest reaction, followed by $k_2 > k_3$.

In the temperature range 42−60 °C, the starting polymer and the polymer obtained after degradation are both above their CP's and therefore in the precipitated state throughout the degradation process. Degradation of the polymer with the monolactate and dilactate side groups shows first-order kinetics in this temperature range. From Table 2 it can be seen that at 60 °C the k_2 and k_3 for the polymer are around ∼10−20 times smaller than those for the monomer, while k_1 for the polymer is ∼100 times smaller than for the monomer. This can be explained by fact that, once the polymer is in its precipitated state, the hydrolyzable ester groups are in a relatively hydrophobic microenvironment. In this environment of low dielectric constant the hydrolysis slows down (Figure 4). Table 2 also shows that at 60 °C the fastest reaction step for the hydrolysis of the lactic acid side groups of the polymer is the one described by k_2 ("backbiting", Scheme 1). This is in contrast to the degradation of the polymer in the soluble state, where the degradation of the ester bond between the two lactate groups is the fastest reaction, as also observed for the monomer. Obviously, the terminal hydroxyl group in the precipitated polymer is still sufficiently mobile to participate in the backbiting reaction, resulting in the cleavage of the lactoyl lactate. When the polymer is in a soluble state, $k_3 < k_1$ (as for the monomer). However, in the precipitated state $k_3 > k_1$. This can be explained by the fact that poly(NIPAAm-*co*-HPMAm-monolactate) has a higher CP than poly(NIPAAm-*co*-HPMAm-dilactate) and is therefore more hydrophilic in the precipitated state. It should be noted that k_1 for the polymer at 60 °C is about the same as k_1 at 15 °C (the monomer shows an increase of a factor 270). This is a unique observation that despite an increase of 45 °C the reaction rate does not increase.

When the incubation temperature is in between the CP's of the starting polymer and the fully hydrolyzed polymer (i.e., from 19 to 40 °C for the polymer with dilactate), then the polymer goes from a precipitated state to a soluble state during hydrolysis. In contrast to the observations of Shah et al.,[40] who reported a change in the degradation kinetics for poly(NIPAAm-*co*-*N*-acryloxysuccinimide) which went from a precipitated to a soluble state due to hydrolysis of the side groups, we found that the polymer degradation followed first-order kinetics.

Above the CP, the (apparent) activation energies for hydrolysis of the ester bond between two lactate groups and the ester bond between the precipitated polymer backbone and lactate are 37 ± 13 kJ/mol. These very low (apparent) activation energies for these two reactions can be explained as follows. Above the CP's two factors counteract each other. First, a higher temperature will result in a higher reaction rate. Second, with increasing temperature, the polymer becomes stronger dehydrated which is associated with a decrease in dielectric constant of the microenvironment of the precipitated polymer. As demonstrated in this paper, the reaction rate decreases with dielectric constant (Figure 4). These counteracting effects result in reaction rate constants that are hardly dependent on temperature and consequently in a low apparent E_a.

Degradation of block copolymers poly(NIPAAm-*co*-HPMAm-mono(di)lactate)/PEG 5000 at 60 °C and at pH 10 results in the same degradation profiles and comparable values of the rate constants k_1, k_2, and k_3 with those obtained for the polymers without the PEG block. It can thus be concluded that the degradation behavior of the block copolymers follows the degradation kinetics and mechanism already discussed for poly(NIPAAm-*co*-HPMAm-lactate). Therefore, knowing the degradation

rate constants gives the possibility to predict the stability of the polymeric micelles based on poly(NIPAAm-*co*-HPMAm-mono(di)lactate)/PEG under physiological conditions. Since the degradation rate of the ester bond between the blocks at 37 °C is almost 5 times slower compared to the degradation rates of the ester bonds in the side chains, these micelles will destabilize upon hydrolysis of the lactic acid side groups due to formation of more hydrophilic poly(NIPAAm-*co*-HPMAm)/PEG as the main degradation product. According to the results presented in Figures 8 and 9, the kinetic model can very well predict the destabilization of polymeric nanoparticles. The ability to predict the stability of the mentioned polymeric micelles is essential for application of these systems for drug delivery purposes.

Conclusions

This study shows that, with the in this paper presented degradation pathways and kinetics, it is possible to predict and control the destabilization time of polymeric micelles based on poly(NIPAAm-*co*-HPMAm-lactate)/PEG polymers under physiological conditions. This is an important feature once the systems are applied for as drug delivery systems.

Acknowledgment. The authors thank Dr. W. J. M. Underberg from the Department of Pharmaceutical Analysis, Faculty of Pharmaceutical Sciences, Utrecht University, for his helpful suggestions.

References and Notes

(1) Jeong, B.; Kim, S. W.; Bae, Y. H. *Adv. Drug Del. Rev.* **2002**, *54*, 37−51.
(2) Molinaro, G.; Leroux, J. C.; Damas, J.; Adam, A. *Biomaterials* **2002**, *23*, 2717−2722.
(3) Jeong, B.; Bae, Y. H.; Kim, S. W. *J. Controlled Release* **2000**, *63*, 155−163.
(4) Johnston, T. P.; Punjabi, M. A.; Froelich, C. J. *Pharm. Res.* **1992**, *9*, 425−434.
(5) Kabanov, A. V.; Batrakova, E. V.; Alakhov, V. Y. *J. Controlled Release* **2002**, *82*, 189−212.
(6) Yamamoto, Y.; Yasugi, K.; Harada, A.; Nagasaki, Y.; Kataoka, K. *J. Controlled Release* **2002**, *82*, 359−371.
(7) Ding, Z.; Chen, G.; Hoffman, A. S. *J. Biomed. Mater. Res.* **1998**, *39*, 498−505.
(8) Matsukata, M.; Aoki, T.; Sanui, K.; Ogata, N.; Kikuchi, A.; Sakurai, Y.; Okano, T. *Bioconjugate Chem.* **1996**, *7*, 96−101.
(9) Gutowska, A.; Bae, Y. H.; Feijen, J.; Kim, S. W. *J. Controlled Release* **1992**, *22*, 95−104.
(10) Kurisawa, M.; Yokoyama, M.; Okano, T. *J. Controlled Release* **2000**, *68*, 1−8.
(11) Chung, J. E.; Yokoyama, M.; Yamato, M.; Aoyagi, T.; Sakurai, Y.; Okano, T. *J. Controlled Release* **1999**, *62*, 115−127.
(12) Roux, E.; Stomp, R.; Giasson, S.; Pézolet, M.; Moreau, P.; Leroux, J.-C. *J. Pharm. Sci.* **2002**, *91*, 1795−1802.
(13) Shin, Y.; Chang, J. H.; Liu, J.; Williford, R.; Shin, Y. K.; Exarhos, G. J. *J. Controlled Release* **2001**, *73*, 1−6.
(14) Heskins, M.; Guillet, J. E. *J. Macromol. Sci., Chem.* **1968**, *A2*, 1441−1455.
(15) Bae, Y. H.; Okano, T.; Kim, S. W. *J. Polym. Sci., Polym. Phys.* **1990**, *28*, 923−936.
(16) Schild, H. G.; Tirrell, D. A. *J. Phys. Chem.* **1990**, *94*, 4352−4356.
(17) Winnik, F. M. *Polymer* **1990**, *31*, 2125−2134.
(18) Winnik, F. M. *Macromolecules* **1990**, *23*, 233−242.
(19) Neradovic, D.; Hinrichs, W. L. J.; Kettenes-van den Bosch, J. J.; Hennink, W. E. *Macromol. Rapid Commun.* **1999**, *20*, 577−581.
(20) Neradovic, D.; Van Nostrum, C. F.; Hennink, W. E. *Macromolecules* **2001**, *34*, 7589−7591.
(21) Larras, V.; Bru, N.; Breton, P.; Riess, G. *Macromol. Rapid Commun.* **2000**, *21*, 1089−1092.
(22) Marin, A.; Muniruzzaman, M.; Rapoport, N. *J. Controlled Release* **2001**, *75*, 69−81.
(23) Nishiyama, N.; Kataoka, K. *J. Controlled Release* **2001**, *74*, 83−94.
(24) Kohori, F.; Yokoyama, M.; Sakai, K.; Okano, T. *J. Controlled Release* **2002**, *78*, 155−163.
(25) Adams, M. L.; Kwon, G. S. *J. Controlled Release* **2003**, *87*, 23−32.
(26) Topp, M. D. C.; Dijkstra, P. J.; Talsma, H.; Feijen, J. *Macromolecules* **1997**, *30*, 8518−8520.
(27) Zhu, P. W.; Napper, D. H. *Langmuir* **2000**, *16*, 8543−8545.
(28) Maeda, Y.; Taniguchi, N.; Ikeda, I. *Macromol. Rapid Commun.* **2001**, *22*, 1390−1393.
(29) Virtanen, J.; Holappa, S.; Lemmetyinen, H.; Tenhu, H. *Macromolecules* **2002**, *35*, 4763−4769.
(30) Wang, L. Q.; Tu, K.; Li, Y.; Fu, J.; Yu, F. *J. Mater. Sci., Lett.* **2002**, *21*, 1453−1455.
(31) Leemhuis, M.; Van Nostrum, C. F.; Van Steenis, J. H.; Hennink, W. E. *Eur. J. Org. Chem.* **2003**, 3344−3349.
(32) Van Dijk-Wolthuis, W. N. E.; Tsang, S. K. Y.; Kettenes-van den Bosch, J. J.; Hennink, W. E. *Polymer* **1997**, *38*, 6235−6242.
(33) Cadée, J. A.; De Kerf, M.; De Groot, C. J.; Den Otter, W.; Hennink, W. E. *Polymer* **1999**, *40*, 6877−6881.
(34) De Jong, S. J.; De Smedt, S. C.; Wahls, M. W. C.; Demeester, J.; Kettenes-van den Bocsh, J. J.; Hennink, W. E. *Macromolecules* **2000**, *33*, 3680−3686.
(35) Van Dijk-Wolthuis, W. N. E.; Van Steenbergen, M. J.; Underberg, W. J. M.; Hennink, W. E. *J. Pharm. Sci.* **1997**, *86*, 413−417.
(36) De Jong, S. J.; Arias, E. R.; Rijkers, D. T. S.; Van Nostrum, C. F.; Kettenes-van den Bosch, J. J.; Hennink, W. E. *Polymer* **2001**, *42*, 2795−2802.
(37) Van de Wetering, P.; Zuidam, N. J.; Van Steenbergen, M. J.; Van der Houwen, O. A. G. J.; Underberg, W. J. M.; Hennink, W. E. *Macromolecules* **1998**, *31*, 8063−8068.
(38) Villermaux, S.; Villermaux, J.; Gibert, R. *J. Chim. Phys.* **1966**, *63*, 1356−1358.
(39) Atkins, P. W. *Physical Chemistry*, 2nd ed.; Oxford University Press: New York, 1982; p 940.
(40) Shah, S. S.; Wertheim, J.; Wang, C. T.; Pitt, C. G. *J. Controlled Release* **1997**, *45*, 95−101.

MA034381N